ORIGINAL RESEARCH

The Therapeutic Effect of iMSC-Derived Small Extracellular Vesicles on Tendinopathy Related Pain Through Alleviating Inflammation: An in vivo and in vitro Study

Zhaochen Zhu [1,2,]*, Renzhi Gao [1,2,]*, Teng Ye [1,2], Kai Feng [1,2], Juntao Zhang [2], Yu Chen [2], Zongping Xie [1], Yang Wang [2]

[1]Department of Orthopaedic Surgery, Shanghai Jiao Tong University Affiliated Sixth People's Hospital, Shanghai, 200233, People's Republic of China; [2]Institute of Microsurgery on Extremities, Shanghai Jiao Tong University Affiliated Sixth People's Hospital, Shanghai, 200233, People's Republic of China

*These authors contributed equally to this work

Correspondence: Zongping Xie, Department of Orthopaedic Surgery, Shanghai Jiao Tong University Affiliated Sixth People's Hospital, 600# Yishan Road, Shanghai, 200233, People's Republic of China Email x91034@qq.com

Background: Tendinopathy is a common cause of tendon pain. However, there is a lack of effective therapies for managing tendinopathy pain, despite the pain being the most common complaint of patients. This study aimed to evaluate the therapeutic effect of small extracellular vesicles released from induced pluripotent stem cell-derived mesenchymal stem cells (iMSC-sEVs) on tendinopathy pain and explore the underlying mechanisms.

Methods: Rat tendinopathy model was established and underwent the injection of iMSC-sEVs to the quadriceps tendon one week after modeling. Pain-related behaviors were measured for the following four weeks. Tendon histology was assessed four weeks after the injection. To further investigate the potential mechanism, tenocytes were stimulated with IL-1β to mimic tendinopathy in vitro. The effect of iMSC-sEVs on tenocyte proliferation and the expression of proinflammatory cytokines were measured by CCK-8, RT-qPCR, and ELISA. RNA-seq was further performed to systematically analyze the related global changes and underlying mechanisms.

Results: Local injection of iMSC-sEVs was effective in alleviating pain in the tendinopathy rats compared with the vehicle group. Tendon histology showed ameliorated tendinopathy characteristics. Upon iMSC-sEVs treatment, significantly increased tenocyte proliferation and less expression of proinflammatory cytokines were observed. Transcriptome analysis revealed that iMSC-sEVs treatment upregulated the expression of genes involved in cell proliferation and downregulated the expression of genes involved in inflammation and collagen degeneration.

Conclusion: Collectively, this study demonstrated iMSC-sEVs protect tenocytes from inflammatory stimulation and promote cell proliferation as well as collagen synthesis, thereby relieving pain derived from tendinopathy. As a cell-free regenerative treatment, iMSC-sEVs might be a promising therapeutic candidate for tendinopathy.

Keywords: tendinopathy, pain relief, extracellular vesicles, iPSC derived MSC

Introduction

Tendinopathy is a prevalent musculoskeletal disorder in athlete and non-athlete populations characterized by pain, swelling, and restricted movement.[1] It frequently occurs in the knee, shoulder, as well as hand. Tendinopathy has a high prevalence and incidence rate in general practice, resulting in detrimental effects on patient's daily life.[1,2] Among various symptoms of tendinopathy, pain is the most prominent and disabling one. Rest, oral nonsteroidal anti-inflammatory drugs (NSAIDs), and physical therapy are frequently used to alleviate pain derived from tendinopathy.[3] However, in some rare cases, more invasive interventions may need to be considered when the patient has failed rehabilitation.[4]

Besides, most researches regarding tendinopathy focus on promoting tendon regeneration or anti-inflammation,[5–7] which lacks direct evidence for alleviating pain. Thus, it is of great value to develop a novel strategy for tendinopathy-related pain.

Inflammation plays a vital role in tendinopathy[8] and is an important mechanism underlying chronic musculoskeletal pain.[9] Traditionally, tendinopathy is considered to be a degenerative disease without inflammation. However, recent research suggests that inflammatory cytokines and immune cells could play critical roles in the pathogenesis of tendinopathy.[10,11] Increasing studies have demonstrated the presence of macrophages, mast cells, T and B lymphocytes in tendinopathy.[12,13] Macrophage-driven inflammatory reaction is an important feature of tendon repair in the early stage, but excessive inflammation is not conducive to tissue repair.[14] Tumor necrosis factor α (TNF-α) is a proinflammatory cytokine involved in the degradation of type I collagen and contributes to tendon degeneration.[15–17] Upon stimulation with TNF-α, production of proinflammation cytokines is elevated, including interleukin (IL)-1β, IL-6, substance P, and nerve growth factor (NGF); these further contribute to tendon degeneration and pain.[18,19] NGF is an essential factor in inducing osteoarthritis and lower back pain.[20,21] Taken together, we hypothesize that inflammation plays a crucial role in the pathogenesis of tendinopathy and related pain. Alleviating inflammation is of great value in the management of tendinopathy pain.

Mesenchymal stem cells (MSCs) have been well investigated in the field of inflammatory diseases as well as autoimmune disorders.[22,23] We recently derived MSC from induced pluripotent stem cell (iPSC) and proved this iMSC to have the same character as adult MSC in function.[24] As iMSC overcomes the limitation of tissue-derived MSC, it is a promising source for stem cell therapy. In recent years, MSCs derived small extracellular vesicles (MSCs-sEVs) have attracted much attention as a novel cell-free strategy in tissue repairing. These 30–150 nm vesicles contain various proteins, nucleic acid, and other biomolecules secreted from parent cells and can transport them to the recipient cells.[25] In our previous research, iMSCs-sEVs were observed to attenuate osteoarthritis by alleviating inflammation and promoting chondrocyte proliferation.[26,27] In addition, MSCs-sEVs have been reported to attenuate inflammatory response after tendon injury and promote tendon regeneration by facilitating tendon stem/progenitor cell proliferation and migration.[28,29] However, there is no report on the application of iMSC-sEVs to alleviate pain derived from tendinopathy to date.

In the present study, we investigated the analgesic effect of iMSCs-sEVs on a rat tendinopathy model and further investigated the potential functional mechanism on IL-1β-induced tenocyte inflammation. It turns out that iMSC-sEVs alleviate inflammation both in vitro and in vivo. iMSC-sEVs treatment was found to upregulate the expression of anti-inflammation-related genes and those that regulate cell proliferation and tenogenic differentiation under high-throughput transcriptome analysis. Here, we show for the first time that iMSC-sEVs possess the potential to ameliorate pain derived from tendinopathy via protecting tenocytes from inflammatory stimulation, at least in part, by inhibiting inflammation and promoting tenocyte proliferation.

Methods
Derivation and Characterization of Induced MSCs
Three human iPSC lines were provided by the Institute of Biochemistry and Cell Biology of the Chinese Academy of Sciences and the South China Institute for Stem Cell Biology and Regenerative Medicine Group of the Chinese Academy of Sciences and used in generation of mesenchymal stem cells. The local ethics committee approved the use of human iPSC in this study of the Shanghai Sixth People's Hospital affiliated with Shanghai Jiao Tong University. The generation of mesenchymal stem cells from human induced pluripotent stem cells as previously described.[30] Surface antigens of iMSCs were analyzed by flow cytometry. Single-cell suspension was collected and incubated with 1% bovine serum albumin (BSA, Gibco). The iMSCs were then stained with the following monoclonal antibodies (BD Bioscience) against CD73, CD90, CD105, CD34, CD45, CD146and HLA-DR. These cells were further analyzed by a CytoFLEX flow cytometer (Beckman Coulter Life Science, USA).

Isolation of iMSC-sEVs

iMSC-sEVs were extracted by centrifugation protocols as previously described[31] from the conditioned medium of iMSC. Briefly, the conditioned medium was collected and centrifuged at 300g for 10 min and 2000g for 20 min to remove cells, dead cells, respectively. Afterward, the supernatant was centrifuged at 10,000g for 30 min and filtered through a 0.22-μm filter sterilize Steritop™ (Millipore) to remove cellular debris and microvesicles. This collected supernatant was subsequently subjected to ultracentrifugation at $100,000 \times g$ for 70 min in an SW 32 Ti Rotor Swinging Bucket rotor (k factor of 256.8, 28536 rpm, Beckman Coulter, Fullerton, CA) to pellet sEVs. After removing the supernatant, the pellet was resuspended in phosphate buffer saline (PBS), followed by another ultracentrifugation at 100,000g for 70 min. Finally, pelleted sEVs were resuspended in PBS stored at −80°C. All steps were performed at 4°C under sterile conditions.

Nano-Flow Analysis of the Size and Concentration of iMSC-sEVs

The size and concentration of iMSC-sEVs were assessed using a nano-flow cytometer (N30 Nanoflow Analyzer, NanofCM Inc., Xiamen, China), as described previously.[32] Briefly, the side scatter intensity (SSI) was measured by loading the standard polystyrene nanoparticles (200 nm) with a concentration of 1.58×10^8/mL to the nano-flow cytometer. Then, the isolated iMSC-sEVs sample was diluted with 1000-fold PBS (the nanoparticle concentration was about 5×10^9/mL) and loaded into the nanofiltration to measure SSI. Finally, the concentration of sEVs was calculated according to the ratio of SSI to particle concentration in standard polystyrene nanoparticles. For size measurement, standard silica nanoparticles of mixed sizes (68 nm, 91 nm, 113 nm, 155 nm) were loaded into a nanometer flow cytometer to generate a standard solution, which was then loaded into the sEVs sample. Size distribution is calculated according to the standard curve.

Identification of Surface Markers of iMSC-sEVs

Three positive markers of iMSC-sEVs, including CD9, TSG101, CD63, and one negative marker GM130, were evaluated to identify sEVs by western blot analysis. Specifically, iMSC-sEVs were collected as described above. The proteins of iMSC-sEVs were harvested using RIPA lysis buffer (Beyotime Biotechnology, China, P0013C) supplemented with protease inhibitor cocktail (Beyotime Biotechnology, China, ST505). Next, the protein concentration of iMSC-sEVs was measured by the Pierce BCA Protein Assay Kit (Beyotime Biotechnology, China, P0012). Protein extracts were resolved by 10% SDS-PAGE and probed with the indicated antibodies. The antibodies against the following proteins were used for western blot analysis: CD63 (1:1000; ab134045, Abcam), CD9 (1:2000; ab92726, Abcam), TSG101 (1:1000; sc-7964, Santa Cruz), GM130 (1:1000; ab52649, Abcam). After three washes with TBST, the membranes were incubated with HRP-conjugated secondary antibodies (1:1000, Cell Signaling Technology, USA) at room temperature for 1 h. The immunoreactive bands were visualized using ECL (Thermo Fisher Scientific, USA, WP20005) and imaged with a FluorChem M Fluorescent Imaging System (ProteinSimple, Santa Clara, CA, USA).

Establishment of Rat Tendinopathy Model

A total of 20 adult female Sprague Dawley rats (200–300 g) were used to develop the tendinopathy model. Rats were randomly assigned to sham or tendinopathy groups with different treatments (PBS, steroid or iMSC-sEVs local injection). The rat tendinopathy model was established as previously reported.[33,34] For this rat tendinopathy model for evaluating pain, we used a variation of carrageenan-induced rat paw edema model in which a single injection of carrageenan solution was made around the quadriceps tendon. The procedure included the following. The carrageenan solution was made by dissolving carrageenan powder (Sigma-Aldrich/Merck KGaA, Darmstadt, Germany) into sterile PBS to make a 4% solution. Briefly, rats were anesthetized with isoflurane, positioned supine, and the fur above the right quadriceps was shaved clean. Then, 100 μL of the 4% carrageenan solution was injected in a single bolus around the right quadriceps tendon with a 27-gauge needle under ultrasound imaging guidance (Fujifilm VisualSonics; Bothell, Washington, USA). The ultrasound probe was a high-frequency 40-MHz linear array

transducer positioned parallel to the femur. We were careful not to damage the tendon with the injection needle physically.

Pain-related behaviors (below) were assessed one week after carrageenan injection and once per week for the following 4 weeks. After 4 weeks of treatment, both quadriceps tendons were harvested following histological evaluation after a lethal overdose of anesthetic. The animal research committee approved animal care and experimental procedures of the Hospital. All the rats were housed under specific-pathogen-free conditions, 12/12-hour light/dark cycle, and free access to food and water.

Pain Measurements

Hind-Paw Withdrawal Threshold

Reflexive measures of pain using stimulus-evoked responses, such as hind-paw withdrawal threshold, are commonly used in rats to assess potential hyperalgesia, and these are thought to reflect clinical expressions of the neuropathic pain.[35] Hind-paw withdrawal thresholds were measured according to a previous report.[36] Briefly, the rats were placed individually in an elevated metal grid cage with sufficient space for them to move their paws while the rest of their body was restricted with plastic plates. After the rats acclimated to the apparatus, the rat's right hind paw withdrawal threshold (PWT) was assessed by an electronic von Frey instrument (model BIO-EVF4; Bioseb, Vitrolles France). The probe tip of the instrument was gently placed perpendicularly into the mid-plantar surface of the paw, and steadily increasing pressure (between 0 and 100 grams) was applied until the hind paw was first lifted. This force is independent of the movements of the limb. The PWT was recorded as the required pressure to first lift the paw. The data were expressed as PWT in grams (g). Lower PWT values (g) were taken as indicators of pain.

Static Weight Bearing

The static weight-bearing (SWB) distribution over the right and left knee was assessed by measuring postural equilibrium between the injected and non-injected leg.[36,37] Briefly, a rat was placed in the chamber of a weight-bearing measuring device (model #BIO-SWB-TOUCH-M; Bioseb) and allowed to acclimate before regular testing. The force applied through each hind limb to the paw resting on the floor of the chamber was measured in grams (g), and an SWB index was calculated as follows:

$$\text{SWB index} = \frac{\text{Force applied to right limb}}{\text{Force applied to right limb} + \text{Force applied to left limb}}$$

The right side received the carrageenan injection. SWBs can vary between 0 and 1, with values closer to zero indicating that postural equilibrium favors the rat's left non-injected side. For each rat, the test was given three times at each assessment period, and the mean value was taken as the SWB at that time point.

Treatments for Tendinopathy-Pain Model

Rats were assigned randomly to four experimental treatment groups (N = 5 per group): (1) sham tendinopathy; (2) PBS-treated tendinopathy (vehicle); (3) iMSC-sEVs-treated tendinopathy; (4) steroid-treated tendinopathy. Sham rats received a PBS injection around the quadriceps tendon. Non-sham rats received a 4% carrageenan injection around the quadriceps tendon to induce tendinopathy. One week later, groups 2–4 received a subsequent injection of iMSC-sEVs (see below) or PBS.

iMSC-sEVs (1×10^{10} particles of iMSC-sEVs in 100 μL PBS) or vehicle (PBS alone, 100 μL) were administered via local injection once a week for 4 weeks. Steroids were prepared by mixing 0.4 mg triamcinolone acetonide (Kunming Jida Pharmaceutical Co., Ltd, Kunming, China) with 100 μL of lidocaine (Shandong Hualu Pharmaceutical Co., Ltd, Shandong, China), which was then injected into the peritendon space of the quadriceps tendon under the ultrasound guidance once a week for 4 weeks. The groups were blinded to the investigators performing behavioral tests and histological assessments. Pain-related behaviors were analyzed each week for the following 4 weeks, after which histological assessment was performed. Reversal (%) of pain-related behaviors was calculated as follows:

$$Reversal\ (\%) = 100\ \times\ \frac{(\text{posttreat value, tendinopathy rats})\ -\ (\text{pretreat value, tendinopathy rats})}{(\text{avg.pretreat value sham rats})\ -\ (\text{pretreat value in tendinopathy rats})}$$

where "value" represents the values for SWB or hind paw withdrawal threshold.

Histology and Immunohistochemistry

For histological analysis, the rat tendon samples were fixed *en bloc* in 4% PFA for 24 hours, dehydrated with a graded ethanol series, embedded in paraffin, and sectioned (5 μm thick) parallel to the long axis of the tendon. One series of sections was mounted on glass slides, cleared with xylene, then hydrated in a graded-ethanol series, stained with hematoxylin and eosin (H&E), and coverslipped. Another series of sections were prepared for immunohistochemical analysis.

We performed immunohistochemistry staining on another series of paraffin-embedded sections to assess the proinflammatory cytokine distribution in rat tendon samples. The following antibodies were used: anti-interleukin-1β (IL-1β) (1:100; ab9722, Abcam), anti-tumor necrosis factor-α (TNF-α) (1:200; ab220210, Abcam), anti-interleukin-6 (IL-6) (1:100; ab9324, Abcam), and anti-nerve growth factor (NGF) (1:200; ab52918, Abcam). HRP-conjugated goat anti-rabbit (Boster Biological Technology, Pleasanton, CA, USA) and HRP-conjugated goat anti-mouse (Boster Biological Technology, Pleasanton, CA, USA) antibodies were used with DAB as the chromogen for visualization. In some cases, a hematoxylin counterstaining was done for nuclear counterstaining.

Histological and immunohistochemical staining was evaluated and photo-documented digitally with Leica digital camera. Image J and modified Bonar system were used for semiquantitative histological analysis as previously reported.[38,39]

Isolation and Culture of Rat Primary Tenocytes

In this study, rat primary tenocytes were isolated from rat Achilles tendon as previously described with minor modification.[40] Briefly, The Achilles tendon was detached from the rat and washed with PBS; the tendon sheath and surrounding paratenon were carefully removed. Afterward, the tendon tissues were cut into small pieces and followed by digestion with 3mg/mL type I collagenase (Invitrogen, Carlsbad, CA, USA) in low-glucose Dulbecco's Modified Eagle's Medium (LG-DMEM) for 3–4h at 37°C. After centrifugation at 1000 revolutions per minute (rpm) for 5 min at room temperature, the digested cells were then suspended in LG-DMEM containing 10% (v/v) fetal bovine serum (FBS, Gibco Life Technologies), 100 U/mL penicillin and 100 mg/mL streptomycin. The cells were incubated in humidified conditions at 37°C and 5% CO2, with media changes every 2 to 3 days. After 10 days, cells started to adhere to the tissue culture flask. When tenocytes reached 80% to 90% confluency, they were treated with 0.05% trypsin–ethylene diamine tetra-acetic acid (EDTA) and passaged. Cells from passage 3 to 5 were used for the subsequent experiments.

Uptake of iMSC-sEVs by Tenocytes in vitro

In the in vitro experiment, iMSC-sEVs were labeled with DiO fluorochrome (Thermo Fisher, USA) according to the protocol as previously described[41] with minor modification. Briefly, sEVs were incubated with DiO fluorescent dye under room temperature for 15 min, followed by ultracentrifugation at 100,000g in PBS to get rid of the unlabeled dye. Next, DiO-labeled sEVs were added into the culture medium and incubated with rat tenocytes for 12h. In the control group, the same volume and concentration of DiO dye without iMSC-sEVs labeling was ultracentrifuged and washed as mentioned above, followed by incubation with tenocytes. Next, the culture medium was discarded, and the cells were rinsed twice with PBS and fixed with 4% PFA. After being stained with DAPI solution, the cells were observed with a fluorescence microscope (Leica, DM6B, Germany).

In vitro Tenocyte Model Mimicking Tendinopathy Condition

IL-1β is significantly upregulated in tendinopathy tissue and is used to mimic conditions in vitro.[42,43] Briefly, before the stimulation of IL-1β, tenocytes were cultured in a medium containing 1% serum for 24h. The medium was then replaced with the medium containing 100 ng/mL recombinant IL-1β (Sigma, St. Louis, MO, USA), 100 ng/mL IL-1β and $1{\times}10^{9}$ p/

mL iMSC-sEVs. The tenocytes were divided into the following three groups (n = 3 per group) according to different treatments: control group (PBS), IL-1β+vehicle group (100 ng/mL IL-1β), and IL-1β+sEVs group (100 ng/mL IL-1β + 1×10^9 p/mL iMSC-sEVs).

Real-Time Quantitative Polymerase Chain Reaction (RT-qPCR) Analysis of Tenocytes

Following treatment of IL-1β with or without iMSC-sEVs for 24h as described above, targeted gene expression analyses were performed by RT-qPCR. Briefly, the total RNA of samples was extracted using EZ-press RNA Purification Kit (EZBioscience, USA). RNA quantity and purity were confirmed with a Nanodrop spectrophotometer (Thermo Scientific, Wilmington, DE). A 4× Reverse Transcription Master Mix (EZBioscience, USA) was used for reverse transcription reaction. PCR reactions were run using the ABI Prism 7900HT Real-Time System (Applied Biosystems, Carlsbad, CA) with 2× SYBR Green qPCR Master Mix (EZBioscience, USA). The primer sequences used in this study are listed in Supplementary Table 1.

Evaluation of Tenocyte Proliferation

The CCK8 assay was used to determine cell viability under iMSC-sEVs treatment. Rat tenocytes (5000 cells/well) were seeded in 96-well plates and cultured with various treatments for 72 hours. At 24, 48 and 72h after the treatments, the cell viability was measured. Briefly, the culture medium was replaced with a medium containing 10% CCK-8 solution. After incubation with CCK-8 solution for 1h at 37°C, absorbance in each well was measured at 450 nm in a microplate reader.

Enzyme-Linked Immunosorbent Assay (ELISA)

We performed ELISA of the culture medium to evaluate the inflammatory factors secreted by the tenocytes. Following treatment of IL-1β with or without iMSC-sEVs for 48h as described above, the culture medium was collected. Interleukin (IL)-1β, tumor necrosis factor (TNF)-α, interleukin (IL)-6, and nerve growth factor (NGF) concentrations were measured by using a rat ELISA kit (Shanghai Westang Bio-Tech Co., LTD., Shanghai, China) according to the manufacturer's instructions. The absorbance was measured by a microplate reader (Thermo Fisher Scientific, Waltham, MA, USA) at 450 nm.

RNA-Seq Analysis

Before constructing the RNA-seq libraries, the total RNA samples (1 μg) of tenocytes were treated with VAHTS mRNA Capture Beads (Vazyme) to enrich polyA+ RNA. RNA-seq libraries were prepared using VAHTS mRNA-seq v2 Library Prep Kit for Illumina (Vazyme) according to the manufacturer's instructions. Briefly, polyA+ RNA samples were fragmented and then used for first- and second-strand cDNA synthesis with random hexamer primers. DNA End Repair Kit was used to repair the ends of the cDNA fragments. The cDNA fragments were then modified with Klenow to add an A at the 3' end of the DNA fragments and ligated to adapters. Twelve cycles of PCR amplification were performed to the purified dsDNA. The libraries were then sequenced by the Illumina sequencing platform on a 150 bp paired-end run. Sequencing reads from RNA-seq data were aligned using the spliced read aligner HISAT2, supplied with the Nov. 2020 (mRatBN7.2/rn7) assembly of the rat genome (rn7, Wellcome Sanger Institute) from UCSC Genome Browser. FPKM (fragments per kilobase of transcript per million mapped reads) was used to calculate the gene expression levels. Gene Set Enrichment Analysis (GSEA) pre-ranked was run on the ranked list using the Molecular Signatures Database (MSigDB) as the gene sets.

Statistical Analysis

All numerical data are presented as means ± SD. Student's *t*-test was used to evaluate paired group differences, and Wilcoxon signed-rank test was used to evaluate nonpaired groups. Statistical analyses were performed with GraphPad Prism version 8.0.0 for Windows (GraphPad Software, San Diego, California, USA). *P* value <0.05 was considered significantly different.

Results

Characterization of iMSC and iMSC-sEVs

In the present study, iPSCs-derived MSC (iMSC) was used to produce therapeutic sEVs in alleviating tendinopathy and related pain. Flow cytometry was applied to evaluate the surface antigen profile of these cells to identify iMSC. iMSC highly expresses antigen markers, including CD73, CD29, CD44, and CD146, but does not express CD34, CD45, CD133, and HLA-DR (Figure 1A). sEVs were isolated and collected from the serum-free culture medium of iMSC by
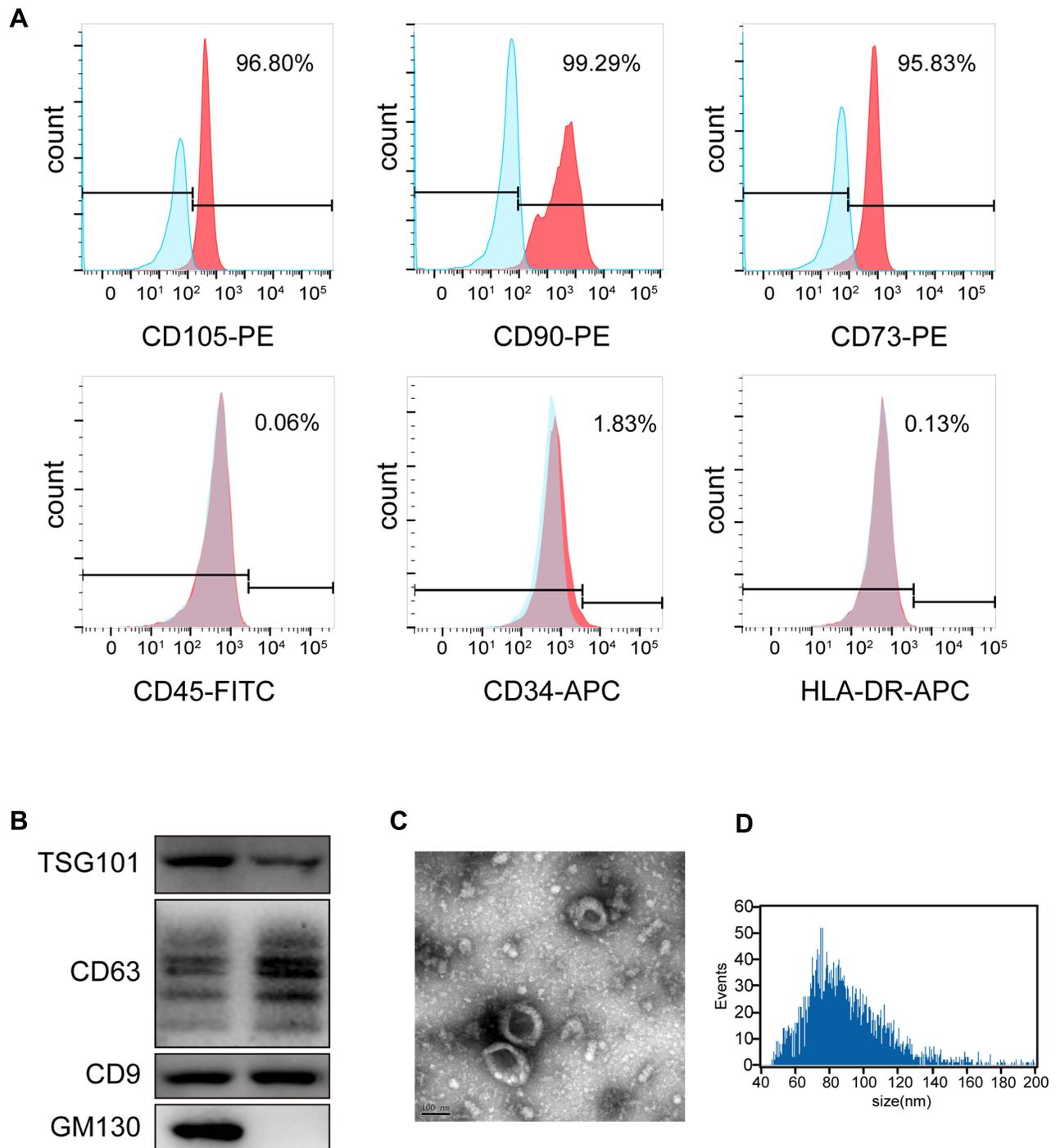

Figure 1 Characterization of iMSC and iMSC-sEVs. (**A**) Surface antigen profile of iMSC evaluated by flow cytometry. (**B**) Western blotting showing the expression of exosomal markers including CD9, TSG101, and CD63 in iMSC-sEVs, but not the negative marker GM130. (**C**) Representative image of iMSC-sEVs observed by TEM. Scale bar = 100 nm. (**D**) Particle size distribution of iMSC-sEVs measured by nano-flow cytometer.

standard differential centrifugation protocol. The iMSC-sEVs pellets were subsequently resuspended with PBS at an approximate concentration of 2×10^{11} particles/mL measured by nano-flow cytometry. After collection, systematic characterization was performed to evaluate the quality of isolated sEVs. Western blot analysis determined the presence of exosomal markers, such as CD9, TSG101, and CD63, whereas the cis-Golgi matrix protein GM130 was not detected (Figure 1B). The morphology of iMSC-sEVs was typical cup-shaped vesicles, as shown by TEM analysis (Figure 1C). Nano-flow analysis revealed that the average diameter of collected sEVs ranges from 60 to 160 nm (Figure 1D).

Analgesic Effect of iMSC-sEVs on a Rat Tendinopathy Model

In order to assess the analgesic effect of iMSC-sEVs on tendinopathy, a rat tendinopathy model was established and subjected to iMSC-sEVs injection a week after the model establishment. Pain-related behaviors were assessed for a total of 5 weeks (Figure 2A). Static weight bearing (SWB) and hind-paw withdrawal thresholds (PWT) are proxy measures of limb pain widely used to quantify knee pain and hyperalgesia in rat models of osteoarthritis.[44] We used these measures to assess the analgesic effect of iMSC-sEVs on pain-related behaviors.

First, in order to inject drugs into the peri-tendon space of the quadriceps tendon, we subjected the following injection procedure under the guidance of ultrasound (Figure 2B and C). After one week after injecting iMSC-sEVs around the tendon, significant PWT and SWB reversal was observed in the iMSC-sEVs group compared with the PBS group. Both SWB and PWT improved gradually within 4 weeks after iMSC-sEVs treatment, and most SWB and PWT measures of pain had significant long-term analgesia, except for SWB at 1 week after treatment (Figure 2D and E).

We further compared the analgesic effect of iMSC-sEVs with an anesthetic combined with a steroid, which are conventional drugs frequently used as a conservative treatment for tendinopathy. Anesthetic and steroids were injected under the same injection protocol as iMSC-sEVs. Both groups have a significant effect in alleviating pain over four weeks. The reversal of hind paw withdrawal threshold and static weight-bearing of the two groups (Figure 2F and G) were statistically indistinguishable.

Thus, chronic pain derived from tendinopathy could be significantly reversed by an injection of iMSC-sEVs solution. The analgesic effect is comparable to anesthetic and steroid injection.

iMSC-sEVs Alleviate Inflammatory Cytokine Infiltration in Tendinopathy Rat Model

In order to investigate the potential mechanism of iMSC-sEVs alleviating pain in the rat tendinopathy model, we performed a complementary experiment with the tendons of rats. Five weeks after model establishment, rat tendon showed the characteristic tendinopathy features, including undulating, disorganized collagen fibers, hypercellularity, increased numbers of round-shaped, darkly stained nuclei, and clusters of capillaries. In contrast, the iMSC-sEVs group appeared less collagen degeneration and cellularity with H&E staining (Figure 3A). Semiquantitative histological analysis showed that the total Bonar score, which includes cell morphology and cellularity was significantly lower in the iMSC-sEVs group than the PBS group (Figure 3B).

CD31 and CD86 is a key marker of vascularity[45] and macrophage (proinflammatory phenotype, M1),[46] respectively. Upon visual inspection, we also observed fewer (visually compared to the PBS group) positively immunostained cells for IL-1β, TNF-α, IL-6, NGF, CD86 and CD31 (Figure 3A). Moreover, quantitative histological analysis of positively stained area percent showed the same trend (Figure 3B). In conclusion, iMSC-sEVs can alleviate inflammation infiltration (inflammatory cytokines and cells), inhibit capillary proliferation and rescue tendon from degenerative status in the rat tendinopathy model according to the histological analysis of the tendon.

iMSC-sEVs Protect Tenocyte from Inflammatory Stimulation

First of all, primary tenocytes were isolated from the rat Achilles tendon and further identified by the expression of Scleraxis and Col I (Figure 4A). In order to determine whether iMSC-sEVs could be internalized by tenocytes, iMSC-sEVs were labeled with Dil fluorescent dye and cocultured with tenocytes isolated above. After 12 hours of incubation, Dil-labeled iMSC-sEVs were efficiently up-taken by tenocytes (Figure 4B).

To further explore the effect of iMSC-sEVs on the function of tenocytes under inflammation conditions, an in vitro tendinopathy model was established by stimulating rat tenocytes with IL-1β. Tenocytes subjected to IL-1β stimulation
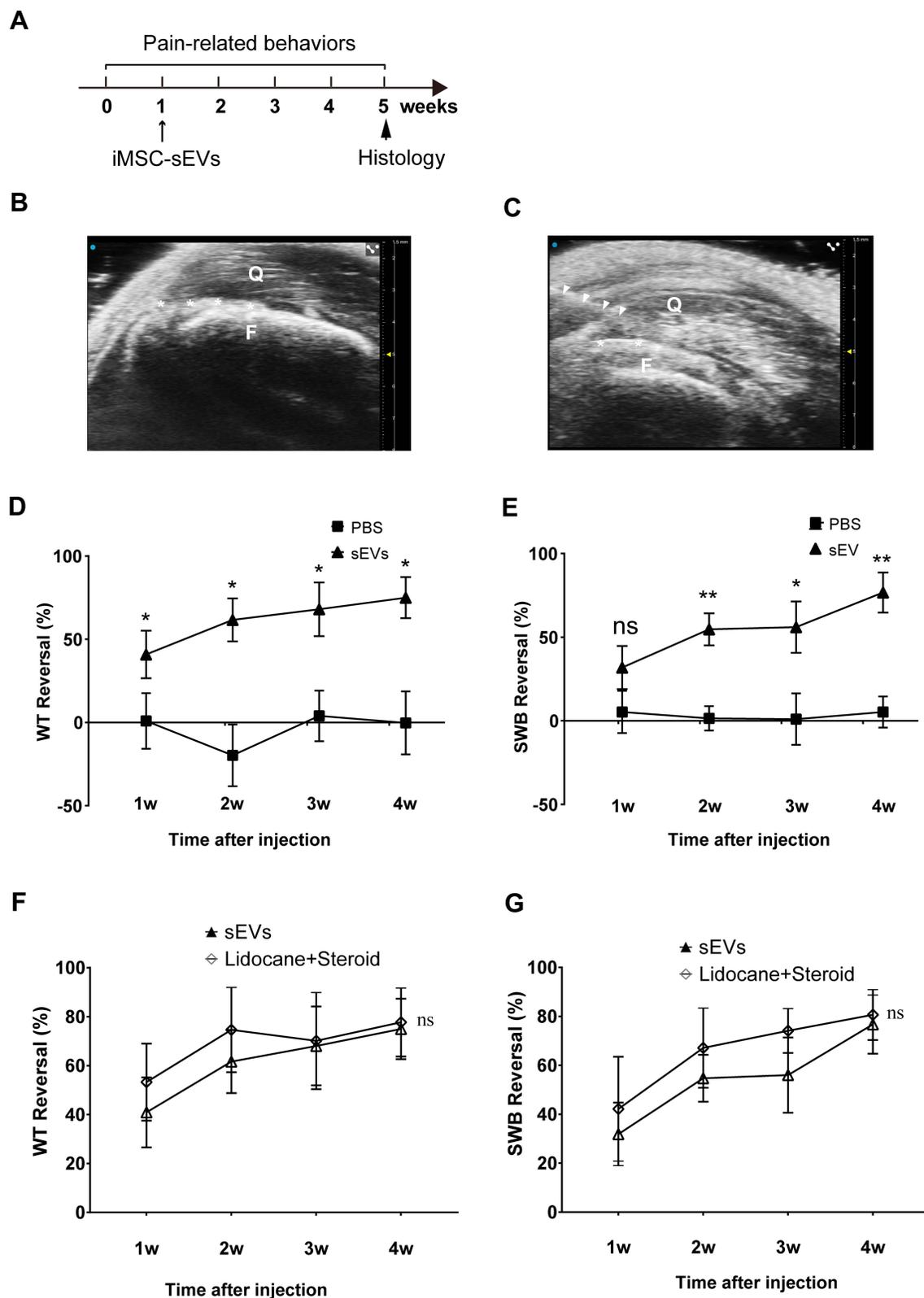
Figure 2 Analgesic Effect of iMSC-sEVs on Rat Tendinopathy Model. (**A**) Diagram showing timing for the model establishment and iMSC-sEVs treatment. Pain-related behaviors were assessed once per week for 5 weeks and histopathological changes were evaluated at 5 weeks after model establishment. (**B**) Ultrasonogram of rat's right leg (anterior view) around the quadriceps tendon showing quadriceps (Q) and femur (F). (**C**) Ultrasonogram showing the relative position of needle (white triangles) used to inject 4% carrageenan (100 μL bolus) solution around the quadriceps tendon. Asterisks (white) in (**B** and **C**) indicate the position of the quadriceps tendon. Pain-related behaviors were performed by using PWT (**D**) and SWB (**E**) reversal (%) up to 4 weeks after tendinopathy model establishment. PWT (**F**) and SWB (**G**) reversal (%) up to 4 weeks after tendinopathy model establishment. N = 5 rats for each group. SWB = static weight bearing; PWT = hind-paw withdrawal threshold; Data are presented as mean ± SD. *P < 0.05. **P < 0.01. ns indicates no significant difference.
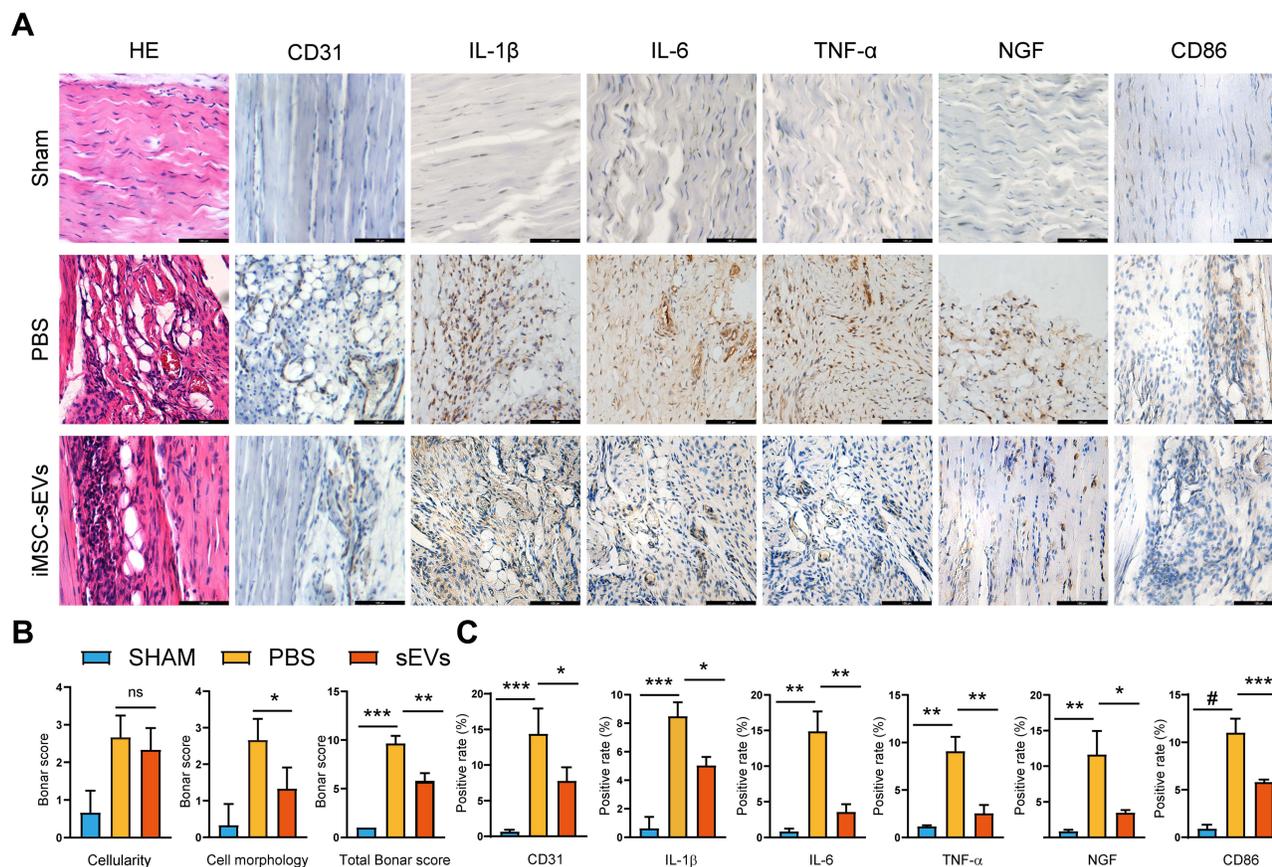
Figure 3 iMSC-sEVs alleviate inflammatory cytokine infiltration in rat tendinopathy model. (**A**) Representative photomicrographs of H&E and immunohistochemically stained tissue sections of different groups at week 5 after model establishment. Positive immunostaining of IL-1β, IL-6, TNF-α, and NGF was visualized with DAB (brown), and nuclei were counterstained with hematoxylin (blue). Scale bar = 100μm. (**B**) Modified Bonar score, including cell morphology and cellularity, is used for semiquantitative histology analysis. C Quantitative analysis of immunohistochemical staining. Data are expressed as mean ± SD. *P < 0.05. **P < 0.01. ***P < 0.001. #P < 0.0001.

exhibited significantly decreased ability of cell proliferation and increased expression of inflammatory mediators as compared to the vehicle group (Figure 4C and D). iMSC-sEVs significantly enhanced the proliferation capability of tenocytes at three days after the iMSC-sEVs intervention when compared to the vehicle treatment (Figure 4C). Besides, decreased expression of inflammatory factors including IL-1β, TNF-α, IL-6, and NGF was also observed in the iMSC-sEVs group, compared to that in the vehicle group 24 h after administration, as shown in Figure 4D.

The secretion of inflammatory factors into the culture medium was also decreased in the iMSC-sEVs group. Upon IL-1β stimulation, significantly increased expression of IL-1β, TNF-α, IL-6, and NGF could be observed in the culture medium of the tenocyte compared with the vehicle group. Compared to the vehicle group, the concentration of TNF-α in the iMSC-sEVs group was significantly decreased (18.1 ± 0.4 pg/mL vs 22.5 ± 0.9 pg/mL [vehicle], P < 0.01). The concentration of IL-1β was statistically indistinguishable from the mean concentration in the vehicle group (45.0 ± 1.0 pg/mL vs 52.9 ± 2.5 pg/mL [vehicle]). The concentration of IL-6 significantly decreased (483.3 ± 9.1 pg/mL vs 532.6 ± 22.1 pg/mL [vehicle], P < 0.01). The concentration of NGF also significantly decreased (788.6 ± 8.6 pg/mL vs 844.4 ± 27.5 pg/mL [vehicle], P < 0.01) (Figure 4E). Collectively, these data indicated that iMSC-sEVs could protect tenocytes from IL-1β stimulation by promoting cell proliferation and resisting the secretion of inflammatory cytokines of tenocytes.

iMSC-sEVs Modulate the Gene Expression Pattern of Rat Tenocytes Under the Stimulation of IL-1β

To explore the underlying molecular mechanism by which iMSC-sEVs rescue tenocytes function, we performed RNA-seq analysis to clarify the changes in gene expression in tenocytes. We applied IL-1β-treated tenocytes with iMSC-sEVs
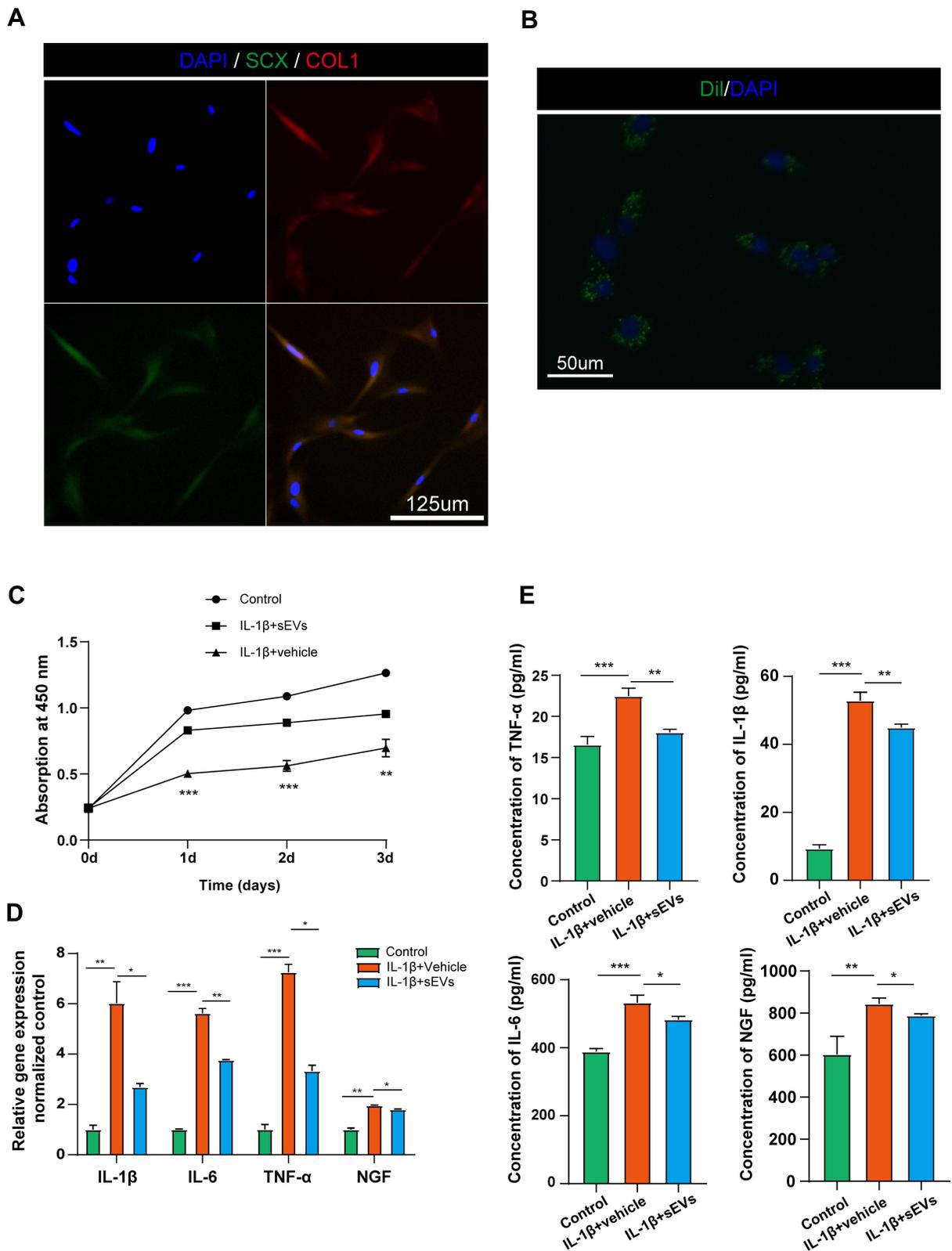
Figure 4 iMSC-sEVs protect tenocytes from IL-1β stimulation. (**A**) Immunofluorescence staining of tenocytes (Scleraxis$^+$, green; Col I$^+$, red). Scale bar = 125μm. (**B**) Immunofluorescence staining of iMSC-sEVs and tenocytes (Dil$^+$, green). Scale bar = 50μm. In the in vitro model of tenocytes inflammation, the proliferation of tenocytes was evaluated by CCK-8 assay (**C**); PCR (**D**) and ELISA (**E**) assays were performed to determine the mRNA and protein levels of IL- 1β, IL-6, TNF-α and NGF. All data are expressed as means ± SD. *P < 0.05, **P < 0.01, ***P < 0.001. All experiments were repeated at least three biological replicates independently.

$(1 \times 10^9$ particles/mL) or PBS for 48 hours. We identified 485 up-regulated genes (> 2-fold, $p < 0.05$) and 379 down-regulated genes (<0.5-fold, $p < 0.05$) after sEVs treatment (Figure 5A). Next, we performed gene set enrichment analysis (GSEA) according to Reactome Knowledgebase (https://reactome.org). The results revealed that many differentially expressed genes were involved in cell proliferation and inflammation (Figure 5B). Specifically, iMSC-sEVs exposure significantly increased the enrichment score for the module of "cell proliferation" (Figure 5C) and "DNA replication" (Figure 5D), while decreased the enrichment score for the module of "interleukin-2 family signaling" (Figure 5E) and "collagen degradation" (Figure 5F) in tenocytes. Genes that showed a significant difference in expression (fold change >2) in the GSEA analysis were visualized by heatmap (Figure 5G and H). Furthermore, RT-qPCR analysis confirmed that the expression of proliferative and anti-inflammatory genes in tenocytes was increased after iMSC-sEVs treatment (Figure 5I). Together, these data clearly revealed that alleviation of inflammation phenotypes in tenocytes after iMSC-sEVs treatment is associated with genetic programs and pathways that control critical aspects of the anti-inflammatory process, cell proliferation, and collagen degradation.

Discussion

In this study, we found that sEVs isolated from iPS-MSCs significantly alleviate pain derived from tendinopathy and reduce inflammation infiltration in a rat tendinopathy model. We further demonstrated that iMSC-sEVs could promote tenocyte proliferation and modulate inflammation conditions under the stimulation of IL-1β. Mechanistically, iMSC-sEVs alleviate pain, in part, via modulation of inflammation, cell proliferation, and collagen degeneration in tendinopathy. Our present study is the first to report that iMSC-sEVs modulate inflammation and alleviate pain derived from tendinopathy.

To date, most efforts have focused on repairing and antiinflammation in tendinopathy. Less attention has been directly paid to the management of pain, which is the most common complaint of patients with tendinopathy.[47] Steroid injections may have good short-term effects in tendinopathy but are known to have side-effect on the long-term perspective,[48] and may even result in tendon rupture after steroid use.[49] In this study, we aimed to investigate novel therapy for pain derived from tendinopathy and further explore the potential mechanism. Firstly, we expanded the use of carrageenan to develop painful quadriceps tendinopathy and observed remarkable increases in pain-related behaviors.

Rats possess advantages over other animals used to model tendinopathy. The rat quadriceps tendon is large enough to be operated on and harvested efficiently, and the limb anatomy of rats is similar to that of humans.[50] In addition, well-established pain-related behaviors can be measured with various inexpensive apparatuses. Carrageenan is a proinflammatory substance that has generally been used in generating acute and chronic pain in the muscle[51] and joints[52] and subcutaneous pain.[53] It represents a consistent and convenient tool in developing animal models of pain and is well studied. In terms of tendinopathy, carrageenan has been applied to induce patella,[33] deep digital flexor,[54] and Achilles[55] tendinopathy. It leads to the deteriorative mechanical and histological changes in the affected tendons.[33,34] Thus, the application of this carrageenan-induced quadriceps tendinopathy model and the pain-related behavior could be generalized in research regarding novel therapies for tendinopathy pain.

iMSC-sEVs have a high potential as cell-free factors for pain management because of their superior functions in the modulation of cell fate and immune response. It has been reported that MSC has an analgesic effect in osteoarthritis[56] and neuropathic pain.[57,58] MSC-derived sEVs were also demonstrated to exert an analgesic effect as they can transport bioactive components, including lipid, protein, as well as RNAs, from the sourced cells to recipient cells. He et al reported that exosomes derived from bone marrow MSC could relieve pain derived from knee OA and protect cartilage damage. Consistently, in this research, iMSC-sEVs were demonstrated to alleviate pain derived from the rat tendinopathy model. Compared with steroids, iMSC-sEV may not have these harmful side effects and can therefore be promising new therapeutics.

An increasing number of studies have confirmed the presence of inflammatory cells and other mediators in chronic tendinopathy. The presence of mediators like MMPs, COX, VEGF, and inflammatory cells indicate that anti-inflammatory compounds may have potential in managing chronic tendinopathy and related pain.[16] MSC-derived sEVs possess the ability to regulate inflammation and immune response. Zhang et al reported that exosomes derived from MSC could alleviate pain in temporomandibular joint osteoarthritis by regulating signal pathways including AKT, ERK, and AMPK.[59] Previously, our team reported the effect of MSC-derived sEVs could attenuate chronic prostatitis/pelvic pain syndrome in the rat by immunoregulation.[60] In terms of osteoarthritis, we demonstrated that iMSCs-sEVs could
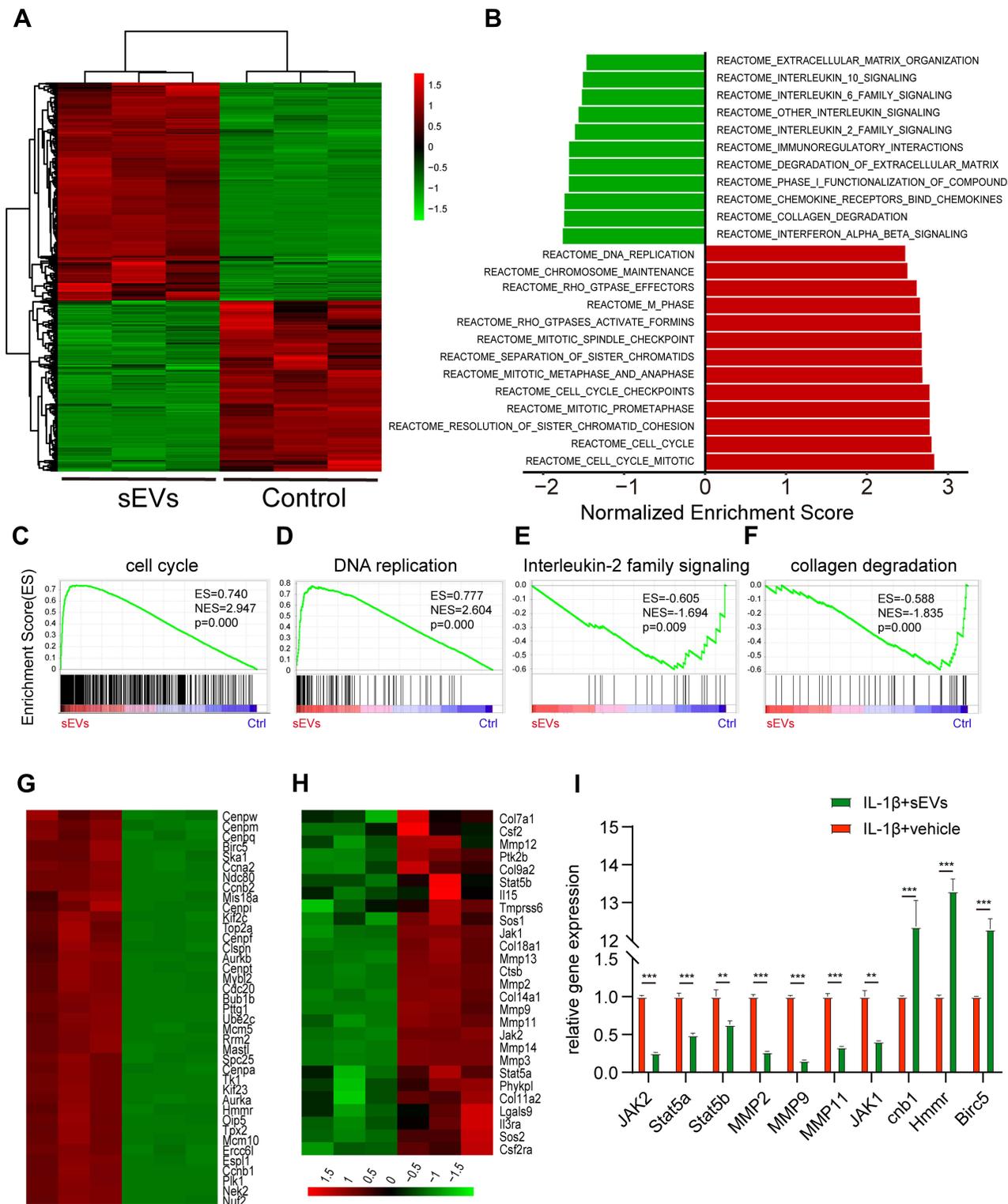
Figure 5 iMSC-sEVs Modulate the Gene Expression Pattern of Rat Tenocytes Under the Stimulation of IL-1β. (**A**) Heatmap representing the hierarchical clustering of significant differential expression genes in rat tenocytes treated with or without iMSC-sEVs. (**B**) GSEA analysis showing canonical pathways of the differentially expressed genes in tenocytes. (**C**–**F**) GSEA analysis identifies enrichment score for modules of cell cycle (**C**), DNA replication (**D**), interleukin-2 family signaling (**E**), and collagen degradation (**F**) in tenocytes after iMSC-sEVs treatment. Heatmap representation of differentially expressed genes (fold change >2) in the GSEA analysis associated with cell cycle (**G**), interleukin-2 family signaling and collagen degradation (**H**). (**I**) RT-qPCR analysis of anti-inflammatory gene expression in tenocytes after iMSC-sEVs treatment. The experiment was repeated three times independently. P-value is indicated as sEVs group versus ctrl group. **P < 0.01, ***P < 0.001.

significantly ameliorate osteoarthritis by suppressing inflammation and promote matrix synthesis.[26] In our present study, significantly decreased expression of inflammatory cytokines and cells was observed in vivo and in vitro after iMSC-sEVs treatment, indicating that iMSC-sEVs may exert an analgesic effect on the tendinopathy rat model mainly by regulating the inflammatory environment within the tendon.

RNA-seq and bioinformatics analysis of sequencing data after iMSC-sEVs treatment identified upregulated genes involved in tenocyte proliferation collagen synthesis, as well as downregulated genes involved in inflammation. This finding is consistent with the therapeutic effect of iMSC-sEVs in protecting tenocytes from inflammatory stimulation and promoting tenocyte proliferation. Moreover, GSEA analysis showed that iMSC-sEVs activated the expression of genes involved in anti-inflammation, cell proliferation and collagen synthesis. Among these genes, Stat5a, Stat5b, Sos2, Sos1, Jak1, Il3ra, Jak2 are associated with the IL-2 family signaling pathway and have been reported to inhibit inflammation of tenocytes.[61–63] Ccnb1, Nek2, Hmmr, Birc5 are cell cycle-related genes that have been demonstrated to promote cell cycle progression, suppress apoptosis and stimulate tendon regeneration.[64–66] In addition, MMP2, MMP9, MMP13 are known to be essential for the collagen degradation of tenocytes and extracellular matrix.[67,68] In conclusion, this evidence suggests that the therapeutic effect of iMSC-sEVs in protecting tenocytes from inflammatory stimulation is credited to the activation of these anti-inflammation, proliferation, and collagen synthesis associated genes.

On the whole, iMSC-sEVs can significantly ameliorate pain derived from tendinopathy, which is attributed to the potency of anti-inflammation, proliferation, and collagen synthesis. iMSC-sEVs have the potential to be translated into the treatment for tendinopathy patients.

Ethical Review Committee Statement

The study protocol was approved by the Ethics Committee of Shanghai JiaoTong University Affiliated Sixth People's Hospital (DWLL2020-0583), and the experimental procedure followed the ethical standards in the Institutional Animal Care and Use Committee of our hospital. All efforts were made to minimize the number and suffering of animals used in this study.

Author Contributions

All authors made substantial contributions to conception and design, acquisition of data, or analysis and interpretation of data; took part in drafting the article or revising it critically for important intellectual content; agreed to submit to the current journal; gave final approval of the version to be published; and agree to be accountable for all aspects of the work.

Funding

Disclosure

The authors report no conflicts of interest in this work.

References

1. Riel H, Lindstrøm C, Rathleff M, Jensen M, Olesen J. Prevalence and incidence rate of lower-extremity tendinopathies in a Danish general practice: a registry-based study. *BMC Musculoskelet Disord*. 2019;20(1):239. doi:10.1186/s12891-019-2629-6
2. De Vries A, Koolhaas W, Zwerver J, et al. The impact of patellar tendinopathy on sports and work performance in active athletes. *Res Sports Med*. 2017;25(3):253–265. doi:10.1080/15438627.2017.1314292
3. Chianca V, Albano D, Messina C, et al. Rotator cuff calcific tendinopathy: from diagnosis to treatment. *Acta Biomed*. 2018;89(1–s):186–196. doi:10.23750/abm.v89i1-S.7022
4. Silbernagel KG, Hanlon S, Sprague A. Current clinical concepts: conservative management of achilles tendinopathy. *J Athl Train*. 2020;55(5):438–447. doi:10.4085/1062-6050-356-19
5. Choi HJ, Choi S, Kim JG, et al. Enhanced tendon restoration effects of anti-inflammatory, lactoferrin-immobilized, heparin-polymeric nanoparticles in an Achilles tendinitis rat model. *Carbohydr Polym*. 2020;241:116284. doi:10.1016/j.carbpol.2020.116284
6. Kang S, Yoon JS, Lee JY, Kim HJ, Park K, Kim SE. Long-term local PDGF delivery using porous microspheres modified with heparin for tendon healing of rotator cuff tendinitis in a rabbit model. *Carbohydr Polym*. 2019;209:372–381. doi:10.1016/j.carbpol.2019.01.017
7. Kim SE, Yun Y-P, Shim K-S, Jeon DI, Park K, Kim H-J. In vitro and in vivo anti-inflammatory and tendon-healing effects in Achilles tendinopathy of long-term curcumin delivery using porous microspheres. *J Ind Eng Chem*. 2018;58:123–130. doi:10.1016/j.jiec.2017.09.016
8. Abate M, Silbernagel K, Siljeholm C, et al. Pathogenesis of tendinopathies: inflammation or degeneration? *Arthritis Res Ther*. 2009;11(3):235. doi:10.1186/ar2723

9. Cazzola M, Atzeni F, Boccassini L, Cassisi G, Sarzi-Puttini P. Physiopathology of pain in rheumatology. *Reumatismo*. 2014;66(1):4–13. doi:10.4081/reumatismo.2014.758

10. Tang C, Chen Y, Huang J, et al. The roles of inflammatory mediators and immunocytes in tendinopathy. *J Orthop Translat*. 2018;14:23–33. doi:10.1016/j.jot.2018.03.003

11. Dean BJ, Gettings P, Dakin SG, Carr AJ. Are inflammatory cells increased in painful human tendinopathy? A systematic review. *Br J Sports Med*. 2016;50(4):216–220. doi:10.1136/bjsports-2015-094754

12. Schubert TE, Weidler C, Lerch K, Hofstädter F, Straub RH. Achilles tendinosis is associated with sprouting of substance P positive nerve fibres. *Ann Rheum Dis*. 2005;64(7):1083–1086. doi:10.1136/ard.2004.029876

13. Millar NL, Hueber AJ, Reilly JH, et al. Inflammation is present in early human tendinopathy. *Am J Sports Med*. 2010;38(10):2085–2091. doi:10.1177/0363546510372613

14. Manning CN, Martel C, Sakiyama-Elbert SE, et al. Adipose-derived mesenchymal stromal cells modulate tendon fibroblast responses to macrophage-induced inflammation in vitro. *Stem Cell Res Ther*. 2015;6(1):74. doi:10.1186/s13287-015-0059-4

15. Qi J, Chi L, Maloney M, Yang X, Bynum D, Banes A. Interleukin-1beta increases elasticity of human bioartificial tendons. *Tissue Eng*. 2006;12 (10):2913–2925. doi:10.1089/ten.2006.12.2913

16. Rees J, Stride M, Scott A. Tendons–time to revisit inflammation. *Br J Sports Med*. 2014;48(21):1553–1557. doi:10.1136/bjsports-2012-091957

17. Spang C, Renström L, Alfredson H, Forsgren S. Marked expression of TNF receptors in human peritendinous tissues including in nerve fascicles with axonal damage - Studies on tendinopathy and tennis elbow. *J Musculoskelet Neuronal Interact*. 2017;17(3):226–236.

18. Takano S, Uchida K, Miyagi M, et al. Nerve growth factor regulation by TNF-α and IL-1β in synovial macrophages and fibroblasts in osteoarthritic mice. *J Immunol Res*. 2016;2016:5706359. doi:10.1155/2016/5706359

19. Nagura N, Kenmoku T, Uchida K, Nakawaki M, Inoue G, Takaso M. Nerve growth factor continuously elevates in a rat rotator cuff tear model. *J Shoulder Elbow Surg*. 2019;28(1):143–148. doi:10.1016/j.jse.2018.06.030

20. Brown M, Murphy F, Radin D, Davignon I, Smith M, West C. Tanezumab reduces osteoarthritic knee pain: results of a randomized, double-blind, placebo-controlled Phase III trial. *J Pain*. 2012;13(8):790–798. doi:10.1016/j.jpain.2012.05.006

21. Markman J, Bolash R, McAlindon T, et al. Tanezumab for chronic low back pain: a randomized, double-blind, placebo- and active-controlled, Phase 3 study of efficacy and safety. *Pain*. 2020;161(9):2068–2078. doi:10.1097/j.pain.0000000000001928

22. Munir H, Ward L, Mcgettrick HM. Mesenchymal stem cells as endogenous regulators of inflammation. *Stromal Immunol*. 2018;4:73–98.

23. Rasmusson I. Immune modulation by mesenchymal stem cells. *Exp Cell Res*. 2006;312(12):2169–2179. doi:10.1016/j.yexcr.2006.03.019

24. Hu GW, Li Q, Niu X, et al. Exosomes secreted by human-induced pluripotent stem cell-derived mesenchymal stem cells attenuate limb ischemia by promoting angiogenesis in mice. *Stem Cell Res Ther*. 2015;6:1–5.

25. Van Niel G, d'Angelo G, Raposo G. Shedding light on the cell biology of extracellular vesicles. *Nat Rev Mol Cell Biol*. 2018;19:213–218.

26. Yang Y, Zhu Z, Gao R, et al. Controlled release of MSC-derived small extracellular vesicles by an injectable Diels-Alder crosslinked hyaluronic acid/PEG hydrogel for osteoarthritis improvement. *Acta Biomater*. 2021;128:163–174.

27. Zhu Y, Wang Y, Zhao B, et al. Comparison of exosomes secreted by induced pluripotent stem cell-derived mesenchymal stem cells and synovial membrane-derived mesenchymal stem cells for the treatment of osteoarthritis. *Stem Cell Res Ther*. 2017;8(1):64. doi:10.1186/s13287-017-0510-9

28. Shen H, Yoneda S, Abu-Amer Y, Guilak F, Gelberman RH. Stem cell-derived extracellular vesicles attenuate the early inflammatory response after tendon injury and repair. *J Orthop Res*. 2020;38(1):117–127. doi:10.1002/jor.24406

29. Yu H, Cheng J, Shi W, et al. Bone marrow mesenchymal stem cell-derived exosomes promote tendon regeneration by facilitating the proliferation and migration of endogenous tendon stem/progenitor cells. *Acta Biomater*. 2020;106:328–341. doi:10.1016/j.actbio.2020.01.051

30. Xia Y, Ling X, Hu G, et al. Small extracellular vesicles secreted by human iPSC-derived MSC enhance angiogenesis through inhibiting STAT3-dependent autophagy in ischemic stroke. *Stem Cell Res Ther*. 2020;11(1):313. doi:10.1186/s13287-020-01834-0

31. Chen B, Sun Y, Zhang J, et al. Human embryonic stem cell-derived exosomes promote pressure ulcer healing in aged mice by rejuvenating senescent endothelial cells. *Stem Cell Res Ther*. 2019;10(1):142. doi:10.1186/s13287-019-1253-6

32. Tian Y, Ma L, Gong M, et al. Protein profiling and sizing of extracellular vesicles from colorectal cancer patients via flow cytometry. *ACS Nano*. 2018;12(1):671–680. doi:10.1021/acsnano.7b07782

33. Eskildsen S, Berkoff D, Kallianos S, Weinhold P. The use of an IL1-receptor antagonist to reverse the changes associated with established tendinopathy in a rat model. *Scand J Med Sci Sports*. 2019;29(1):82–88. doi:10.1111/sms.13310

34. Da Ré Guerra F, Vieira C, Marques P, Oliveira L, Pimentel E. Low level laser therapy accelerates the extracellular matrix reorganization of inflamed tendon. *Tissue Cell*. 2017;49(4):483–488. doi:10.1016/j.tice.2017.05.006

35. Mogil J. Animal models of pain: progress and challenges. *Nat Rev Neurosci*. 2009;10(4):283–294. doi:10.1038/nrn2606

36. Otis C, Gervais J, Guillot M, et al. Concurrent validity of different functional and neuroproteomic pain assessment methods in the rat osteoarthritis monosodium iodoacetate (MIA) model. *Arthritis Res Ther*. 2016;18:150. doi:10.1186/s13075-016-1047-5

37. Malfait A, Little C, McDougall J. A commentary on modelling osteoarthritis pain in small animals. *Osteoarthritis Cartilage*. 2013;21(9):1316–1326. doi:10.1016/j.joca.2013.06.003

38. Cong GT, Lebaschi AH, Camp CL, et al. Evaluating the role of subacromial impingement in rotator cuff tendinopathy: development and analysis of a novel murine model. *J Orthop Res*. 2018;36(10):2780–2788. doi:10.1002/jor.24026

39. Jensen EC. Quantitative analysis of histological staining and fluorescence using ImageJ. *Anat Rec*. 2013;296(3):378–381. doi:10.1002/ar.22641

40. Xiao M, Leonardi EA, Sharpe O, et al. Soaking of autologous tendon grafts in vancomycin before implantation does not lead to tenocyte cytotoxicity. *Am J Sports Med*. 2020;48(12):3081–3086. doi:10.1177/0363546520951815

41. Wiklander OP, Nordin JZ, O'Loughlin A, et al. Extracellular vesicle in vivo biodistribution is determined by cell source, route of administration and targeting. *J Extracell Vesicles*. 2015;4:26316. doi:10.3402/jev.v4.26316

42. Tsuzaki M, Guyton G, Garrett W, et al. IL-1 beta induces COX2, MMP-1, −3 and −13, ADAMTS-4, IL-1 beta and IL-6 in human tendon cells. *J Orthop Res*. 2003;21(2):256–264. doi:10.1016/S0736-0266(02)00141-9

43. Maeda E, Kuroyanagi K, Ando Y, Matsumoto T. Effects of substrate stiffness on morphology and MMP-1 gene expression in tenocytes stimulated with Interleukin-1β. *J Orthop Res*. 2020;38(1):150–159. doi:10.1002/jor.24403

44. Piel MJ, Kroin JS, van Wijnen AJ, Kc R, Im H-J. Pain assessment in animal models of osteoarthritis. *Gene*. 2014;537(2):184–188. doi:10.1016/j.gene.2013.11.091

45. Yang M, Li CJ, Sun X, et al. MiR-497~195 cluster regulates angiogenesis during coupling with osteogenesis by maintaining endothelial Notch and HIF-1α activity. *Nat Commun*. 2017;8:16003. doi:10.1038/ncomms16003

46. Wang C, Zhang Y, Zhang G, Yu W, He Y. Adipose stem cell-derived exosomes ameliorate chronic rotator cuff tendinopathy by regulating macrophage polarization: from a mouse model to a study in human tissue. *Am J Sports Med*. 2021;49(9):2321–2331. doi:10.1177/03635465211020010

47. Smith B, Selfe J, Thacker D, et al. Incidence and prevalence of patellofemoral pain: a systematic review and meta-analysis. *PLoS One*. 2018;13(1):e0190892. doi:10.1371/journal.pone.0190892

48. Everhart JS, Cole D, Sojka JH, et al. Treatment options for patellar tendinopathy: a systematic review. *Arthroscopy*. 2017;33(4):861–872. doi:10.1016/j.arthro.2016.11.007

49. Halpern AA, Horowitz BG, Nagel DA. Tendon ruptures associated with corticosteroid therapy. *West J Med*. 1977;127(5):378–382.

50. Lebaschi A, Deng X, Zong J, et al. Animal models for rotator cuff repair. *Ann N Y Acad Sci*. 2016;1383(1):43–57. doi:10.1111/nyas.13203

51. Berberich P, Hoheisel U, Mense S. Effects of a carrageenan-induced myositis on the discharge properties of group III and IV muscle receptors in the cat. *J Neurophysiol*. 1988;59(5):1395–1409. doi:10.1152/jn.1988.59.5.1395

52. Radhakrishnan R, Moore S, Sluka K. Unilateral carrageenan injection into muscle or joint induces chronic bilateral hyperalgesia in rats. *Pain*. 2003;104(3):567–577. doi:10.1016/S0304-3959(03)00114-3

53. Rivot J, Montagne-Clavel J, Besson J. Subcutaneous formalin and intraplantar carrageenan increase nitric oxide release as measured by in vivo voltammetry in the spinal cord. *Eur j Pain*. 2002;6(1):25–34. doi:10.1053/eujp.2001.0268

54. Vieira C, De Aro A, Da Ré Guerra F, De Oliveira L, De Almeida MS, Pimentel E. Inflammatory process induced by carrageenan in adjacent tissue triggers the acute inflammation in deep digital flexor tendon of rats. *Anat Rec*. 2013;296(8):1187–1195. doi:10.1002/ar.22729

55. Çınar B, Çirci E, Balçık C, Güven G, Akpınar S, Derincek A. The effects of extracorporeal shock waves on carrageenan-induced Achilles tendinitis in rats: a biomechanical and histological analysis. *Acta Orthop Traumatol Turc*. 2013;47(4):266–272. doi:10.3944/AOTT.2013.2784

56. Matas J, Orrego M, Amenabar D, et al. Umbilical cord-derived mesenchymal stromal cells (MSCs) for knee osteoarthritis: repeated MSC dosing is superior to a single MSC dose and to hyaluronic acid in a controlled randomized Phase I/II trial. *Stem Cells Transl Med*. 2019;8(3):215–224. doi:10.1002/sctm.18-0053

57. Di Cesare Mannelli L, Tenci B, Micheli L. Adipose-derived stem cells decrease pain in a rat model of oxaliplatin-induced neuropathy: role of VEGF-A modulation. *Neuropharmacology*. 2018;131:166–175. doi:10.1016/j.neuropharm.2017.12.020

58. Siniscalco D, Giordano C, Galderisi U. Long-lasting effects of human mesenchymal stem cell systemic administration on pain-like behaviors, cellular, and biomolecular modifications in neuropathic mice. *Front Integr Neurosci*. 2011;5:79. doi:10.3389/fnint.2011.00079

59. Zhang S, Teo KYW, Chuah SJ, Lai RC, Lim SK, Toh WS. MSC exosomes alleviate temporomandibular joint osteoarthritis by attenuating inflammation and restoring matrix homeostasis. *Biomaterials*. 2019;200:35–47. doi:10.1016/j.biomaterials.2019.02.006

60. Peng X, Guo H, Yuan J, et al. Extracellular vesicles released from hiPSC-derived MSCs attenuate chronic prostatitis/chronic pelvic pain syndrome in rats by immunoregulation. *Stem Cell Res Ther*. 2021;12(1):198. doi:10.1186/s13287-021-02269-x

61. Wang Y, He G, Tang H, et al. Aspirin inhibits inflammation and scar formation in the injury tendon healing through regulating JNK/STAT-3 signalling pathway. *Cell Prolif*. 2019;52(4):e12650. doi:10.1111/cpr.12650

62. Surbek M, Tse W, Moriggl R, Han X. A centric view of JAK/STAT5 in intestinal homeostasis, infection, and inflammation. *Cytokine*. 2021;139:155392. doi:10.1016/j.cyto.2020.155392

63. Kato A. Group 2 innate lymphoid cells in airway diseases. *Chest*. 2019;156(1):141–149. doi:10.1016/j.chest.2019.04.101

64. Xie B, Wang S, Jiang N, Li JJ. Cyclin B1/CDK1-regulated mitochondrial bioenergetics in cell cycle progression and tumor resistance. *Cancer Lett*. 2019;443:56–66. doi:10.1016/j.canlet.2018.11.019

65. Fry AM, O'Regan L, Sabir SR, Bayliss R. Cell cycle regulation by the NEK family of protein kinases. *J Cell Sci*. 2012;125(Pt 19):4423–4433. doi:10.1242/jcs.111195

66. Horning AM, Wang Y, Lin CK, et al. Single-cell RNA-seq reveals a subpopulation of prostate cancer cells with enhanced cell-cycle-related transcription and attenuated androgen response. *Cancer Res*. 2018;78(4):853–864. doi:10.1158/0008-5472.CAN-17-1924

67. Van Doren SR. Matrix metalloproteinase interactions with collagen and elastin. *Matrix Biol*. 2015;44–46:224–231. doi:10.1016/j.matbio.2015.01.005

68. Panwar P, Butler GS, Jamroz A, Azizi P, Overall CM, Brömme D. Aging-associated modifications of collagen affect its degradation by matrix metalloproteinases. *Matrix Biol*. 2018;65:30–44. doi:10.1016/j.matbio.2017.06.004